Supplement to One Thousand Years of Mediterranean Silver Trade to the Levant: A Review and Synthesis of Analytical Studies, Journal of Archaeological Research, Tzilla Eshel*, Yigal Erel, Naama Yahalon-Mack, and Ayelet Gilboa.

* Corresponding author: Zinman Institute of Archaeology, University of Haifa
Email: teshel@univ.haifa.ac.il

Materials and Methods

The 19 hoards sampled throughout our project are listed in Table I in the main text, which also includes ingots from the Iron Age IIC ʿUza fortress—though these were found in loose form, rather than as a hoard—and several silver items from an MB III tomb in Megiddo (Eshel et al., in press). Sampling permissions and current locations of the hoards are specified in Eshel 2020, Appendix B.

Chronology

Radiocarbon dating was obtained from the textile wrapping of silver bundles of two hoards, from Tell Keisan (Eshel et al. 2021) and Arad (Eshel et al. 2022a). These were considered alongside a previously published radiocarbon result obtained from the bundle of the Megiddo area H silver hoard (Arie et al. 2019). Most of the silver hoards, however, could not be dated directly. In some cases, dating relied on radiocarbon dates obtained from relevant strata (e.g., Tel Dor; Gilboa and Sharon 2003; Sharon et al. 2007). In others, dating was based on the reassessments of the stratigraphy and the individual context of the hoard, including the up-to-date chronology of the ceramics from the layers in which the hoards were found, and the typology of the containers in which the hoards were cached. Often, personal communications with the excavators, especially regarding unpublished sites, was also part of the inquiry (Eshel et al. 2018; 2019; 2021; 2022a; 2023; Eshel n.d.).

Regarding the correlation between relative and absolute chronology of the Bronze and Iron Ages in the Levant—a much debated topic, radiocarbon dating has been instrumental in solving debates, or narrowing chronological gaps (e.g., for the Iron Age see Shalvi and Gilboa 2023, supplementary material). The terminologies for relative chronology and absolute dates adopted in this and in our previous publications are as follows. For the Middle Bronze Age III (previously termed MB IIC, Greenberg 2019, p. 181), we refer to the two current chronological stances, which reflect the gap between historical events and the radiocarbon dates that are ca. 50 years later: ~1700/1650–1600/1550 BC (Eshel et al. 2023). The Late Bronze Age I–II, accordingly, is dated to ~1600/1550–1200 BC. A unique MB/LB transitional phase was identified at Tell el-ʿAjjul (~1600–1550 BC; Fischer 2021). For the very end of the Late Bronze Age and the Iron Age, we employ the terminology used at Megiddo (Toffolo et al. 2014), and divide this timespan into the following periods: Late Bronze Age III (LB III; ~1200–1150 BC), Early and Late Iron Age I (~1150–1050 BC and ~1050–950 BC, respectively), Early Iron Age IIA (~950–900 BC), Late Iron Age IIA (~900–800 BC), Iron Age IIB (~800–730 BC) and Iron Age IIC (~730–600 BC); (for absolute chronology see: Finkelstein et al. 2013, p. 17, Table 1.1; Gilboa et al. 2015, Table 2; 2018; Shalvi and Gilboa 2023, Table S1; Sharon 2014). In the eighth century BC, radiocarbon dating becomes largely ineffective due to the Hallstatt Plateau in the calibration curve, and from this century onward, dates are assigned on the basis of historical considerations. The end of the Iron IIB in Israel is usually associated with Tiglath-pileser III's campaigns between 734–732 BC, but this ceramic vista most probably continued to a certain extent for several decades later (Fantalkin and Tal 2015, pp. 192, 195; Shalvi and Gilboa 2022a; 2022b). Finally, the termination of the Iron Age in the Levant is usually correlated with Babylonian destructions ca. 600/586 BC (Zorn 2014).

Chemical Composition

Silver objects derived from a single ore source can vary in chemical composition, depending on the heterogeneity of the ore and the production process. Most metals that occur naturally in the lead ore are largely removed from the silver during the cupellation process and concentrate in the litharge. An experiment showed that tin (Sn) and antimony (Sb) are almost entirely removed from silver and taken up by the litharge, while copper (Cu), bismuth (Bi) and lead (Pb) are partially separated from silver during cupellation, often depending on the quality of the process (Pernicka and Bachmann 1983). Therefore, the concentrations of these elements in silver items offer little help in identifying the ore (Albarède et al. 2012; Pernicka 2017), but as detailed below, they might be useful in other respects, including the identification of post-production alloying with other metals. This is especially important when Pb is contributed to the alloy through the addition of metals other than silver, affecting the Pb-isotope values.

Gold (Au) is potentially the most telling element for the chemical characterization of silver sources since it is present in each Ag-rich lead ore at a rather well-defined concentration-range (Craddock 2014; Gale and Stos-Gale 1981b; Meyers 2003; González de Canales et al. 2008; Philip and Rehren 1996; Rehren et al. 1996; Wood et al. 2019; 2020). However, although Au/Ag ratios generally remain unchanged throughout the various stages of lead ore processing and silver production (Meyers 2003; Pernicka and Bachmann 1983), we have shown that in some cases Au was added to silver artefacts through alloying (Eshel et al., 2018; 2019; see below). Accumulating chemical analysis of silver artifacts suggests that Au concentrations do not exceed 1 wt.% (Meyers 2003).

Copper (Cu) alloying with silver found in the Levant is of special interest, as the local Cu ores in the Arabah (Timna and Faynan) contain significant amounts of lead (~1%– 5%; Hauptmann 2007). This may affect the Pb-isotope ratios of the alloy (see more below). Experiments have demonstrated that only some of the copper content of raw lead is removed during cupellation, and therefore Cu concentrations in silver are dependent both on Cu concentrations in the ore, and on the quality of the cupellation process, and may reach up to 2.5 wt.% Cu in the silver, and more (Pernicka and Bachmann 1983, Figs. 2, 3). As there is no clear threshold for Cu alloying, the presence of measurable Ni, Zn, Sb, As and/or Sn in the metal, which should have been easily oxidized and removed during cupellation (Pernicka and Bachmann 1983), is used to identify post- production addition of Cu, namely alloying.

To conclude, trace element concentrations in silver items offer little help in identifying the source of the silver. However, minor elements (Pb, Cu, Au and Bi) which were not fully separated during the cupellation process, can be used in order to identify and differentiate between idiosyncrasies resulting mainly from the production process and later biography. Therefore, these elements are considered below. Significantly, Au and Cu are useful in identifying alloying, which may affect the isotopic results.

Sample preparation, chemical analysis, and lead isotope analysis (LIA; see below) were described in Eshel et al., 2019. Detailed chemical compositions of the silver were measured using an ICP-MS (Agilent 7500cx). The results were obtained via sample drilling, revealing the composition of the items' core, rather than their surface, with high accuracy (margin of error is within the range of a few ppm [parts per million]).

Lead Isotope Analysis

Lead isotope analysis (LIA) is customarily used for sourcing silver. It compares Pb-isotope ratios of artifacts with those of ores and is based on cumulative studies which established that Pb does not undergo significant fractionation during the production process. In our study, we considered all the isotopic data of lead ores available to us, including data from Iberia, Sardinia, Cévennes-France, the Aegean (Laurion in Attica, Siphnos and other Aegean Islands), Anatolia-Taurus, Iran and more (see main text). An R-based application was developed in order to compare the Pb-isotopic compositions obtained from ores in these and other regions to those of the artifacts, enabling us to determine which ores are consistent isotopically with our results.

Although lead isotope analysis is a powerful tool, it does have two major limitations: mixing and ore-overlap (e.g., Gale 2009; Knapp 2000; Pernicka 2014; Pollard 2009; Stos-Gale and Gale 1982). By mixing we mean that Pb-isotope ratios of silver artefacts might reflect a mixture of more than one ore-source. This may be the result of the following processes: (a) Smelting of Pb-poor silver-rich ores, for example, jarosite-rich ores in Iberia that require the addition of lead for the extraction of silver. Thus, the isotopic ratios of the produced silver point mainly to the sources of lead, rather than silver (Eshel et al. 2019). This, however, may be less detrimental to the question of provenance, since the added lead would usually originate from the vicinity of the silver ore or from the same broad region. (b) Alloying silver with other metals such as Pb-rich copper, to improve workability and hardness of the alloy, or as a means of debasement (Eshel et al. 2021). (c) Recycling, when silver scrap, possibly of several origins, is re-melted to produce new objects (e.g., Eshel et al. 2018).

Ore-overlap reflects a situation in which different lead ores have similar geological histories and settings and consequentially similar isotopic compositions. This is the case with some of the major Mediterranean lead ore deposits, such as Laurion in Greece, which overlap several deposits in Anatolia (Gale and Stos-Gale 1981b; Stos-Gale and Gale 1982). In some specific cases, chemical composition (e.g., Au in silver, Pb in copper) and geological characteristics can be used as independent factors to differentiate between ores (Albarède et al. 2012; Baron et al. 2014; L'Héritier et al. 2015; Meyers 2003; Pollard and Bray 2015). Ambiguities can also be resolved through archaeological and historical considerations.

In order to improve the differentiation between ores with overlapping compositions, we use all four lead isotopes and apply them in a manner which reflects the geological histories and settings of the ores, including Pb-isotope growth curves that consider initial Pb isotopic values, U and Th concentrations (expressed as $^{238}U/^{204}Pb$ (μ), $^{232}Th/^{238}U$ (κ)) and the model age of the ore (Stacey and Kramers 1975; see full explanation for the implementation in archaeology in Eshel et al. 2019, S1). The measured values of ores (obtained from the literature) and Pb ratios of silver items from the Levantine hoards are overlaid on top of the model-calculated isochron lines and growth curves. The ores are not homogeneous with respect to U/Pb and Th/Pb, and therefore an ore might have several μ and κ values, which create lines of Pb-isotope ratios, forming the range of ratios that characterize the ore (Albarède et al. 2012; 2020; Pernicka et al. 1993). In some cases, ores appear to fall in the future, an indication that the two-stage model does not fully capture the complexity of ore-formation processes (Hofmann 1997; 2008). In recent years, the geological model became mainstream in archaeometallurgy, and was further developed (Albarède et al. 2012; 2020; 2021; Gentelli et al. 2021). Among these developments are numeric representations of model ages, μ and κ, which contribute additional graphic representations of the data (Albarède et al. 2012).

Large data-sets of silver compositions, such as those available for the Levantine silver hoards, also enable us to overcome some of the above-mentioned limitations, since silver in each hoard shares the same depositional date, and, as we argue below, the lion's share of the items within each hoard are largely contemporary. This enables us in some cases to differentiate between two categories of isotopic ratios of lead in the examined silver artifacts: (a) Endmembers. These are groups of items with similar isotopic compositions, which cluster at opposite sides of the Pb-isotope graphs. Ideally, each cluster is plotted along a unique isochron, clearly representing one specific ore source (see figures below). The clusters may be consistent with ores represented in the databases, but may also represent an unknown or unsampled source (for unknown silver sources see for example Hauptmann et al. 2002 and more below). (b) Mixed and unidentified artifacts. The isotopic ratios of these items fall between the endmembers, and they either reflect the mixing of sources represented by the endmembers, or a contribution from additional sources. Such artefacts, which may contain lead contributions from different sources, are likely to create mixing lines on the graphs, crossing several isochrons (e.g., Eshel et al. 2021, Fig. 7), and we cannot determine whether they represent additional ore sources rather than a mixture of the endmembers.

To conclude, although LIA has several limitations, we demonstrate that silver sources *can* often be positively traced (Eshel et al. 2019; 2021; 2022a; 2023). Correct provenancing depends, nonetheless, not only on high quality data but also on methodology, and therefore considering precise contexts and chronology, chemical composition, mixing and geological constraints, are all essential prerequisites to trace the sources of silver.

Pb-isotopic compositions were measured with a MC-ICP-MS (Thermo Neptune Plus). In previous studies (Eshel et al. 2019; 2021; 2022a; 2023) we compared our isotopic results to the results obtained from some of the same silver hoards by Stos-Gale (OXALID). While some of the results were similar, several outliers were identified in the OXALID data, probably due to fractionation (see above). Here we present only the results obtained by our group. We also consider here for the first time Pb-isotope ratios of silver-rich Pb ores that have only recently been published (Milot et al. 2021; Vaxevanopoulos et al. 2022) and therefore were not considered in previous publications.

Results

Chronology

All the sampled hoards and their relative and absolute dates are listed in Table I in the main text. The specific content, contexts, radiocarbon dating, typology of the items and other considerations which helped to determine the chronology of the hoards and of the items in them were presented in our previous publications (Eshel et al. 2018; 2019; 2021; 2022a; 2023). Assigning most of the hoards to specific centuries and often even to sub-century time spans was crucial for the identification of temporal trends in silver sources and trade during the Bronze and Iron Ages.

Chemical Composition

The general average and median of Cu, Au, Pb and Bi through time, based on the chemical compositions of all 239 silver artefacts sampled, are displayed in Table SI and Figures S1 a–d. The results show a dramatic increase in Cu concentrations in silver items during the LB III (~1200–1150 BC; Figure S1a) and lower but still high concentrations during the Iron Age I (~1150–950 BC). Au average is uniquely high in the Early Iron Age IIA (~950 BC; Figure S1b). Pb concentrations generally did not change with time, except for a significant increase during the Iron Age IIC (~680 BC; Figure S1c). Bi concentrations are relatively high during the Iron Age IIB (~800–730 BC; Figure S1d). Detailed chemical compositions are available in Eshel et al., 2019; 2021; 2022a; 2023.

Table SI: Average and standard deviation of Pb, Bi, Au and Cu concentrations in south Levantine silver sampled in previous studies (Eshel et al. 2019; 2021; 2022; 2023).

Sub period	Average BCE	Hoards	Number of samples	Cu ppm		Au ppm		Pb ppm		Bi ppm	
				average	stdev	average	stdev	average	stdev	average	stdev
MB IIC	1600	Megiddo tomb, Gezer, Shiloh	16	33965	16124	505	448	4754	3058	1789	633
MB/LB	1500	Tell el-ʻAjjul	12	44487	20572	66	163	3958	1221	2258	2437
LB II	1300	Abel Beth Maacah	7	20435	11617	348	310	2450	1673	607	735
LB III	1200	Megiddo Area H, Beth Shean 88866	26	433270	282283	1397	4747	2703	3905	473	651

Iron Age I	1100	Beth Shean 1095, Tell Keisan, Megiddo 2012, Ashkelon	48	185092	132410	881	1758	2573	2825	192	329
Early Iron Age IIA	950	Beth Shean 1029, Dor, ʻAkko	61	21028	14162	18224	31617	5053	7718	935	1833
Late Iron Age IIA	850	ʻEin Hofez	29	8921	5500	205	500	12244	17803	5999	7839
Iron Age IIB	750	Eshtemoa, ʻArad fortress	28	15451	10844	302	1135	5218	7006	6198	3810
Iron Age IIC	680	ʻUza, ʻEin Gedi	12	45701	11936	65	47	33224	12451	1406	609

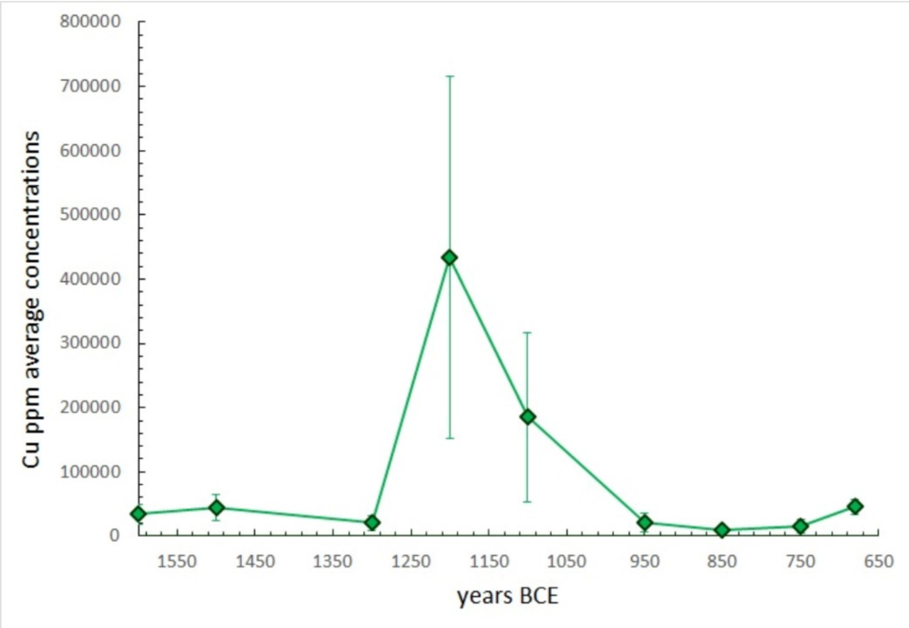

a

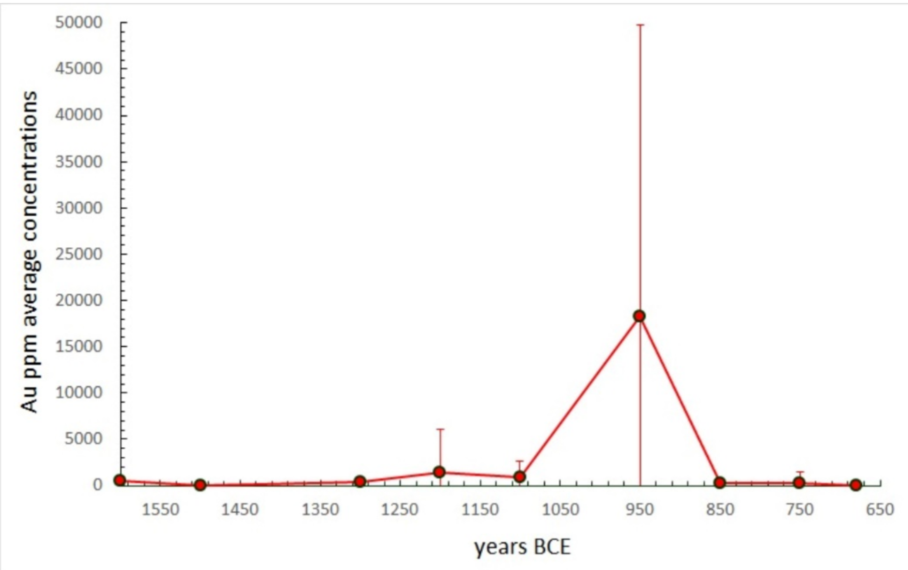

b

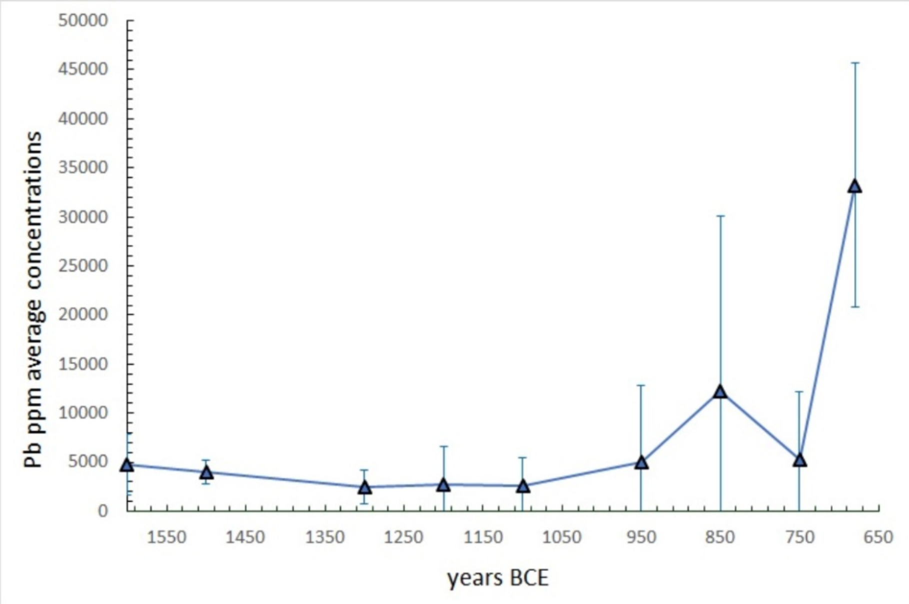

c

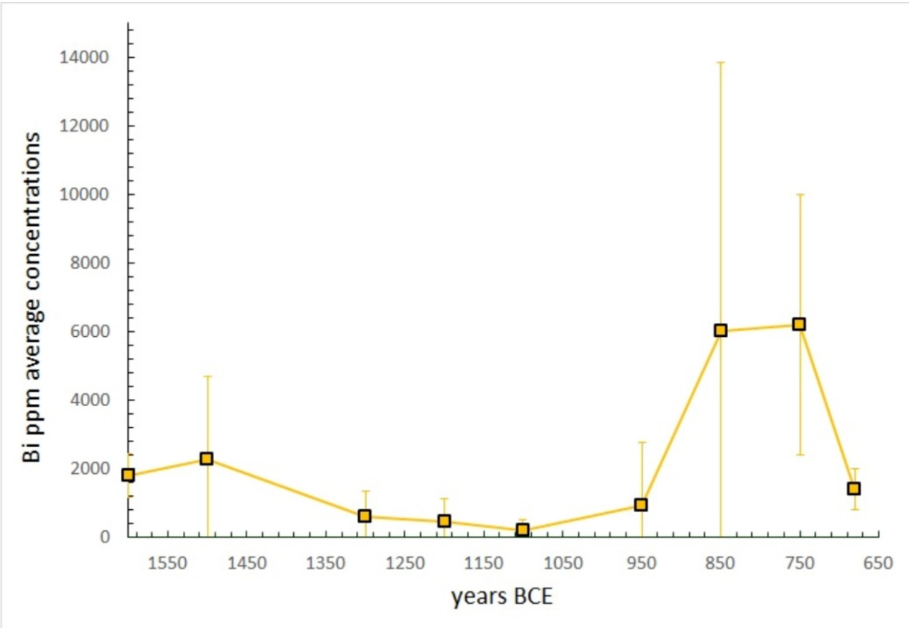

d

Figure S1: Average metal concentrations and standard deviations in silver items, as a function of the different chronological sub periods outlined in this paper (represented here in years BCE). (a) Green rhombus – Cu; (b) Red circles– Au; (c) Blue triangles – Pb; (d) Yellow squares– Bi.

Silver-copper (Ag-Cu) Alloys

All six hoards from the LB III–Iron Age I sequence (~1200–950 BC; from Beth Shean, Megiddo, Tell Kesian and Ashkelon), contained silver with high copper contents (>5.5 wt.%) and trace elements associated with copper, demonstrating that silver was systematically debased by Cu alloying (Eshel et al. 2021). In all other hoards, Cu concentrations in silver usually range between 0.2 wt.% and 6 wt.%, and indicative trace elements are generally not detected (<30 µg/g in most items). From time periods before and after the LB III–Iron Age I, a few samples with elevated Cu concentrations and indicative trace elements suggest sporadic mixing of Ag with Cu rather than systematic debasement (Eshel et al. 2019; 2022a; 2023). In the LB III–Iron Age I hoards, arsenic (As) was intentionally added to some of the Ag-Cu alloys, giving them a silvery tint. We suggested that this was done to conceal the fact that the silver was debased and that both protocols (debasement and the addition of arsenic) indicate a shortage in silver, which resulted from the disruption of trade routes with Late Bronze Age collapse (Eshel et al. 2021). Significantly, the addition of copper to the silver may introduce extraneous lead which would affect the Pb-isotopic composition of the metal (Eshel et al. 2021; see below).

Silver-gold (Ag-Au) Alloys

One hoard, from Tel Dor (Early Iron Age IIA), has several items with elevated Au concentrations, reaching up to 30 wt.%. Clearly such levels are beyond the natural concentrations of Au in Galena, indicating that the silver must have been alloyed with gold (Eshel et al. 2019). For all other hoards, including those of the Early Iron Age IIA (from ʿAkko and Beth Shean), Au concentrations do not exceed 1 wt.% (and are mostly below 0.5 wt%). In a few hoards, sporadic items were found to be Au-rich (Au>1 wt.%; e.g., in the Iron Age II hoards of Beth Shean 1029 a and b, and ʿEin Hofez), probably due to the re-melting of electrum jewelry (Eshel et al. 2018, p. 215, Fig. 13; Eshel n.d.). In contrast to copper, alloying silver with gold is not expected to alter lead isotopic composition of the metal (see more below).

Alloying Ag with Au is generally unlikely, since gold is valued more than silver. This is true also for gold-rich Egypt; Although silver was valued more than gold during the Old Kingdom period in Egypt, it was regarded as less valuable than gold from the Middle Kingdom period onwards (roughly equivalent to the Middle Bronze Age in the Levant; e.g., Gouda et al. 2007; Schorsch 2001). Nonetheless, silver's value versus gold remined high in Egypt during the New Kingdom (~LBA; 2:1 ratio). Given the preceding long period of shortage in silver, the alloying of the silver in the Dor hoard with gold may therefore be explained by the unusually close ties between Dor and Egypt during the Iron Age I and Early Iron Age IIA (Gilboa 2015).

Lead (Pb) concentrations

An exceptionally high concentration of Pb (on average) is evident in the Iron Age IIC (3.3 wt.%), coinciding with a shift of silver sources at this time (Eshel et al. 2022a and below). In other periods, there is no significant change in *average* Pb concentrations with time, however there is a difference in the *range* (standard deviation) of the concentrations. Most Bronze Age and Iron Age I samples have Pb concentrations that range between 0.1 and 1 wt. %, while Iron Age IIA–B samples have a wider range of Pb concentration, with several items having more than 1% Pb, or less than 0.1% Pb (Table S1, Figure S1c). The higher standard deviation (<1 wt.%) during the Iron Age IIA–B may be related to the predominant Phoenician exploitation of jarosites in Iberia during this time, which required the deliberate addition of lead. However, this remains to be examined through experimentation.

Bismuth (Bi) Concentrations

Bi concentrations are elevated during the Late Iron Age IIA and Iron Age IIB (~900–730 BCE; Figure S1d). As nearly all silver in these periods originated from Iberia, this is possibly also related to the exploitation of Jarosites and the addition of external Pb as part of the silver production process (Eshel et al. 2019; 2022a). It has been shown that Bi is released from the ore to the litharge only at the end of the cupellation process (Pernicka and Bachmann 1983). It is possible that the addition of Pb during production in Iberia prevented the metalworkers from reaching a full cupellation process, leaving the Bi in the silver.

The results of the chemical analyses of the silver emphasize the importance of incorporating chemical data in the study of silver sources. Specifically, the deliberate addition of Cu, which may introduce lead into the alloy, affects the Pb-isotopic composition and therefore identifying this addition is a perquisite for proper interpretation of Pb isotopes values (see more below).

Lead Isotope Analysis

Results, presented for the eight sub-periods examined, are available in Table SII. They show, first and foremost, that in each period the isotopic composition of the silver is different.

Table SII: Pb-isotopic ratios of the analysed silver items. For uncertainties and full chemical data see Eshel et al. 2019; 2021; 2022a; 2023).

Period	Hoard	Sample	Type	$^{206}Pb/^{204}Pb$	$^{207}Pb/^{204}Pb$	$^{208}Pb/^{204}Pb$
Middle Bronze Age III (~1700/1650–1600/1550 BC)	**Megiddo Tomb**	Meg tomb 1	pin	18.862	15.688	39.037
		Meg tomb 3	pin	18.886	15.687	39.069
	Gezer	Gezer 1	sheet	18.886	15.682	39.056
	Shiloh	Shiloh 1	cut ingot	18.923	15.692	39.128
		Shiloh 2	cut ingot	18.858	15.685	38.988
		Shiloh 3	cut ingot	19.046	15.722	39.348
		Shiloh 4	cut ingot	18.927	15.701	39.148
		Shiloh 5	cut ingot	18.85	15.682	39.010
		Shiloh 6	cut ingot	18.858	15.677	38.892
		Shiloh 7	square rod	18.91	15.688	39.076
		Shiloh 8	cut ingot	18.851	15.678	38.846
		Shiloh 9	rod	18.918	15.692	39.106
		Shiloh 10	earring	18.906	15.69	39.091
Middle Bronze Age III/ Late Bronze Age I transition (~1600/1550–1500 BC)	**Tell el-'Ajjul 1299**	'Ajjul 1299_3	rod	18.736	15.656	38.719
		'Ajjul 1299_11	rod	18.815	15.684	38.956
		'Ajjul 1299_12	rod	18.781	15.677	38.873
	Tell el-'Ajjul 1312	'Ajjul 1312_1	rod	18.855	15.684	38.938
		'Ajjul 1312_2	rod	18.898	15.689	39.063
		'Ajjul 1312_3	rod	18.815	15.684	38.911
		'Ajjul 1312_4	rod	18.762	15.661	38.836
		'Ajjul 1312_6	rod	18.841	15.682	38.958
		'Ajjul 1312_5	rod	18.779	15.672	38.776
		'Ajjul 1312_7	sheet	18.802	15.673	38.837

		‘Ajjul 1312_9	sheet	18.797	15.679	38.845
		‘Ajjul 1312_10	sheet	18.676	15.629	38.63
Late Bronze Age IIB (~1300–1200 BC)	**Abel Beth Maacah**	ABM 1	earring	18.781	15.674	38.829
		ABM 6	earring	18.766	15.678	38.839
		ABM 12	cut ingot	18.594	15.681	38.704
		ABM 7	cut ingot	18.812	15.688	38.877
		ABM 9	rod	18.88	15.688	38.968
		ABM 10	cut rod	18.817	15.69	38.935
		ABM 11	ingot	18.838	15.678	38.823
Late Bronze Age III (~1200–1150 BC)	**Megiddo H**	Megiddo H_13*	rod	18.298	15.651	38.408
		Megiddo H_14*	cut ingot	18.183	15.640	38.279
		Megiddo H_15*	rod	18.778	15.680	38.834
		Megiddo H_21*	rod	18.309	15.650	38.416
		Megiddo H_22*	rod	18.205	15.651	38.313
		Megiddo H_24*	rod	18.261	15.648	38.364
		Megiddo H_25*	rod	18.310	15.647	38.411
		Megiddo H_26*	rod	18.775	15.684	38.841
		Megiddo H_27*	rod	18.305	15.692	38.432
		Megiddo H_28*	rod	18.039	15.626	38.136
		Megiddo H_29*	square ingot	18.241	15.648	38.347
		Megiddo H_30*	droplet	18.347	15.656	38.436
		Megiddo H_33*	sheet	18.380	15.658	38.472
	Beth Shean 88866	BS 88866_2	rod	18.857	15.689	38.957
		BS 88866_4	earring	18.861	15.684	38.964
		BS 88866_6*	braclet	18.679	15.679	38.754
		BS 88866_7	toggle pin	18.815	15.682	38.854
		BS 88866_13	rod	18.857	15.686	38.952
		BS 88866_15	rod	18.861	15.691	38.968
		BS 88866_19	earring	18.733	15.678	38.869
		BS 88866_24_coating*	cut ingot	18.686	15.677	38.753
		BS 88866_24_core*	cut ingot	18.679	15.679	38.751
		BS 88866_25_core*	cut ingot	18.686	15.677	38.759
		BS 88866_25_coating*	cut ingot	18.698	15.678	38.770
		BS 88866_27_coating*	cut ingot	18.683	15.668	38.727
		BS 88866_27_core*	cut ingot	18.677	15.678	38.747
Iron Age I (~1150–950 BC)	**Beth Shean 1095**	BS 1095_1*	cut ingot	18.725	15.690	38.811
		BS 1095_2*	cut ingot	18.577	15.663	38.527
		BS 1095_3	token	18.687	15.661	38.695
		BS 1095_4*	token	18.421	15.695	38.541
		BS 1095_5*	cut ingot	18.119	15.624	38.066
		BS 1095_6*	cut ingot	18.557	15.648	38.433
	Tell Keisan	Keisan 2_15*	token	18.397	15.660	38.486
		Keisan 2_2*	cut ingot	18.341	15.653	38.315
		Keisan 2_25*	rod	18.488	15.660	38.455
		Keisan 2_4*	cut ingot	18.575	15.666	38.516

		Keisan 2_40*	cut ingot	18.786	15.678	38.719
		Keisan 2_46*	cut ingot	18.539	15.665	38.477
		Keisan 2_49*	cut ingot	18.386	15.686	38.384
		Keisan 2_8*	sheet	18.483	15.665	38.458
		Keisan 6_17*	cut ingot	18.399	15.688	38.406
		Keisan 6_18*	token	18.912	15.684	38.974
		Keisan 6_26*	rod	18.351	15.672	38.339
		Keisan 6_27*	rod	18.262	15.667	38.226
		Keisan 6_28*	wire (jewerly)	18.501	15.677	38.470
		Keisan 6_55*	rod	18.596	15.670	38.535
		Keisan 8_29*	sheet	18.198	15.661	38.324
		Keisan 8_33*	earring	18.312	15.654	38.279
		Keisan 8_37*	sheet	18.441	15.661	38.417
		Keisan 8_4*	cut ingot	18.439	15.659	38.416
		Keisan 8_59*	token	18.837	15.679	38.787
	Megiddo 2012	Megiddo 2012_1*	cut ingot	18.512	15.676	38.602
		Megiddo 2012_2*	cut ingot	18.552	15.664	38.534
		Megiddo 2012_3*	cut ingot	18.718	15.684	38.801
		Megiddo 2012_4*	cut ingot	18.639	15.670	38.747
		Megiddo 2012_5*	rod	18.768	15.677	38.840
		Megiddo 2012_6*	cut ingot	18.437	15.653	38.418
		Megiddo 2012_7*	cut ingot	18.641	15.669	38.583
		Megiddo 2012_8*	cut ingot	18.717	15.664	38.664
		Megiddo 2012_9*	cut ingot	18.685	15.679	38.757
		Megiddo 2012_10*	cut ingot	18.520	15.665	38.518
		Megiddo 2012_11*	cut ingot	18.438	15.668	38.537
	Ashkelon	Ashkelon_1	cut ingot	18.464	15.668	38.522
		Ashkelon_2*	cut ingot	18.706	15.684	38.796
		Ashkelon_3	cut ingot	18.518	15.661	38.514
		Ashkelon_4		18.227	15.649	38.226
		Ashkelon_5*	cut ingot	18.487	15.688	38.581
		Ashkelon_6*	rod	18.659	15.678	38.735
		Ashkelon_7	cut ingot	18.826	15.692	38.904
		Ashkelon_8*	sheet	18.677	15.678	38.763
		Ashkelon_9	sheet	18.451	15.667	38.555
		Ashkelon_10*		18.745	15.682	38.817
		Ashkelon_11*		18.792	15.694	38.933
		Ashkelon_12		18.748	15.689	38.832
Iron Age IIA (~950–800 BC)	**Beth Shean 1029 a+b**	BS 1029_1	rod	18.583	15.665	38.672
		BS 1029_2	cut ingot	18.957	15.698	39.018
		BS 1029_3	ingot	18.669	15.675	38.738
		BS 1029_4	ingot	18.921	15.678	38.943
		BS 1029_5	ingot	18.960	15.703	39.034
		BS 1029_6	ingot	18.652	15.678	38.718
		BS 1029_7	rod	18.790	15.678	38.850
		BS 1029_8	cut ingot	18.989	15.701	39.050
		BS 1029_9	cut ingot	18.808	15.683	38.878

		BS 1029_10	cut ingot	18.703	15.696	38.826
		BS 1029_11	cut ingot	18.875	15.668	39.015
		BS 1029_12	cut ingot	18.940	15.689	38.976
		BS 1029_13	cut ingot	18.983	15.697	39.038
		BS 1029_14	cut ingot	18.522	15.679	38.638
		BS 1029_15	token	18.980	15.692	39.015
	ʽAkko	ʽAkko-1	cut ingot	18.976	15.691	39.015
		ʽAkko-2	cut ingot	18.964	15.688	39.003
		ʽAkko-3	cut ingot	18.957	15.685	38.984
		ʽAkko-4	cut ingot	18.967	15.687	39.003
		ʽAkko-5	cut ingot	17.894	15.633	37.966
		ʽAkko-6	cut ingot	18.030	15.660	38.150
		ʽAkko-7	cut ingot	18.257	15.672	38.374
		ʽAkko-8	cut ingot	18.380	15.688	38.522
		ʽAkko-9	cut ingot	18.661	15.697	39.023
		ʽAkko-10	cut ingot	18.662	15.691	38.821
		ʽAkko-11	cut ingot	18.855	15.675	39.036
		ʽAkko-12	cut ingot	18.709	15.644	38.969
Early Iron Age IIA (~950–900 BC)	**Tel Dor**	Dor-1	cut ingot	18.987	15.702	39.043
		Dor-2	cut ingot	18.971	15.694	39.023
		Dor-3	cut ingot	18.981	15.703	39.053
		Dor-4	cut ingot	18.988	15.695	39.029
		Dor-5	cut ingot	18.976	15.695	39.028
		Dor-6	cut ingot	17.910	15.645	38.003
		Dor-7	cut ingot	17.940	15.645	38.033
		Dor-8	cut ingot	17.910	15.639	37.988
		Dor-9	cut ingot	17.906	15.643	37.991
		Dor-10	cut ingot	18.472	15.685	38.607
		Dor-11	cut ingot	18.177	15.651	38.256
		Dor-12	cut ingot	18.445	15.682	38.560
		Dor-13	cut ingot	18.551	15.696	38.762
		Dor-14	cut ingot	18.553	15.670	38.657
		Dor-15	cut ingot	19.034	15.732	39.382
		Dor-16	cut ingot	18.683	15.676	38.756
		Dor-17	cut ingot	18.612	15.700	38.773
		Dor-18	cut ingot	18.703	15.678	38.905
		Dor-19	cut ingot	18.889	15.688	38.947
		Dor-20	cut ingot	18.648	15.693	38.773
		Dor-21	cut ingot	18.866	15.691	38.917
		Dor-22	cut ingot	18.697	15.681	38.797
		Dor-23	cut ingot	18.827	15.685	38.916
		Dor-24	cut ingot	18.870	15.687	39.035
		Dor-25	cut ingot	18.922	15.686	38.993
		Dor-26	cut ingot	18.915	15.680	38.970
		Dor-27	cut ingot	18.801	15.678	38.837
		Dor-28	cut ingot	18.762	15.714	38.891
		Dor-29	cut ingot	18.896	15.676	38.974

		Dor-30	cut ingot	18.642	15.687	38.757
		Dor-31	cut ingot	18.684	15.678	38.755
		Dor-32	cut ingot	18.649	15.700	39.014
		Dor-33	cut ingot	18.860	15.684	39.026
		Dor-34	cut ingot	18.651	15.706	38.818
Late Iron Age IIA (~900–800 BC)	**‛Ein Hofez**	Hofez-1	cut ingot	18.952	15.694	39.050
		Hofez-2	cut ingot	18.944	15.687	38.981
		Hofez-3	cut ingot	18.214	15.620	38.309
		Hofez-4	cut ingot	18.299	15.636	38.428
		Hofez-5	cut ingot	18.215	15.609	38.331
		Hofez-6	cut ingot	18.180	15.600	38.280
		Hofez-7	cut ingot	18.220	15.614	38.305
		Hofez-8	cut ingot	18.188	15.609	38.303
		Hofez-9	cut ingot	18.325	15.613	38.408
		Hofez-10	cut ingot	18.416	15.632	38.547
		Hofez-11	cut ingot	18.563	15.653	38.683
		Hofez-12	cut ingot	18.509	15.686	38.625
		Hofez-13	cut ingot	18.390	15.632	38.518
		Hofez-14	cut ingot	18.451	15.645	38.582
		Hofez-15	cut ingot	18.448	15.635	38.551
		Hofez-16	cut ingot	18.502	15.644	38.632
		Hofez-17	cut ingot	18.381	15.629	38.461
		Hofez-18	cut ingot	18.356	15.621	38.455
		Hofez-19	cut ingot	18.431	15.625	38.521
		Hofez-20	cut ingot	18.420	15.625	38.540
		Hofez-21	cut ingot	18.405	15.626	38.479
		Hofez-22	cut ingot	18.470	15.640	38.561
		Hofez-23	cut ingot	18.360	15.628	38.463
		Hofez-24	cut ingot	18.679	15.660	38.813
		Hofez-25	cut ingot	18.504	15.641	38.640
		Hofez-26	cut ingot	18.523	15.648	38.651
		Hofez-27	wire	18.423	15.626	38.504
		Hofez-28	wire	18.387	15.622	38.478
		Hofez-29	wire	18.397	15.625	38.493
Late Iron Age IIA–IIB (~900–640/630 BC)	**Eshtemoa**	Eshtemoa_1	cut ingot	18.418	15.646	38.565
		Eshtemoa_2	cut ingot	18.184	15.599	38.233
		Eshtemoa_3	cut ingot	18.715	15.666	38.873
		Eshtemoa_4	cut ingot	18.202	15.615	38.350
		Eshtemoa_7	cut ingot	18.662	15.674	38.731
		Eshtemoa_8	cut ingot	18.471	15.647	38.579
		Eshtemoa_10	cut ingot	18.298	15.615	38.387
		Eshtemoa_11	cut ingot	18.113	15.611	38.233
		Eshtemoa_12	cut ingot	18.269	15.613	38.359
		Eshtemoa_13	cut ingot	18.415	15.640	38.541
		Eshtemoa_14	cut ingot	18.455	15.637	38.564
		Eshtemoa_15	cut ingot	18.358	15.628	38.481
	‘Arad fortress	‘Arad_2_1	cut ingot	18.342	15.666	38.522

		ʻArad_2_2	cut ingot	18.335	15.668	38.520
		ʻArad_2_3	cut ingot	18.335	15.671	38.519
		ʻArad_2_4	cut ingot	18.331	15.665	38.510
		ʻArad_2_8	cut ingot	18.349	15.668	38.526
		ʻArad_2_10	cut ingot	18.397	15.667	38.579
		ʻArad_2_11	cut ingot	18.570	15.686	38.798
		ʻArad_2_19	cut ingot	18.339	15.665	38.520
		ʻArad_2_20	cut ingot	18.734	15.689	38.912
		ʻArad_2_109	wires	18.616	15.665	38.772
		ʻArad_2_119	fragments of jewelry	18.520	15.652	38.602
		ʻArad_2_122	cut ingot	18.441	15.665	38.606
		ʻArad_2_123	cut ingot	18.535	15.684	38.760
		ʻArad_2_132	cut token	18.433	15.676	38.632
		ʻArad_2_133	fragments of jewelry	18.665	15.693	38.807
		ʻArad_2_134	fragments of jewelry	18.465	15.650	38.579
Iron Age IIC (~640/630–600)	**ʻUza ingot**	ʻUza_16_382	ingot	18.696	15.687	38.932
	ʻEin Gedi	ʻEin Gedi_29	cut thick square ingot	18.336	15.667	38.512
		ʻEin Gedi_15	ingot	18.855	15.682	38.865
		ʻEin Gedi_7	ingot	18.841	15.680	38.853
		ʻEin Gedi_17	ingot	18.813	15.681	38.858
		ʻEin Gedi_14	cut ingot	18.840	15.678	38.835
		ʻEin Gedi_8	cut ingot	18.703	15.682	38.921
		ʻEin Gedi_6	cut ingot	18.843	15.683	38.876
		ʻEin Gedi_13	cut ingot	18.842	15.680	38.852
		ʻEin Gedi_26	cut ingot	18.857	15.683	38.867
		ʻEin Gedi_3	cut ingot	18.697	15.681	38.878
		ʻEin Gedi_18	cut ingot	18.700	15.682	38.908

*Ag-Cu alloys, the isotopic composition is expected to be affected by Cu addition (see more in Eshel et al. 2021).

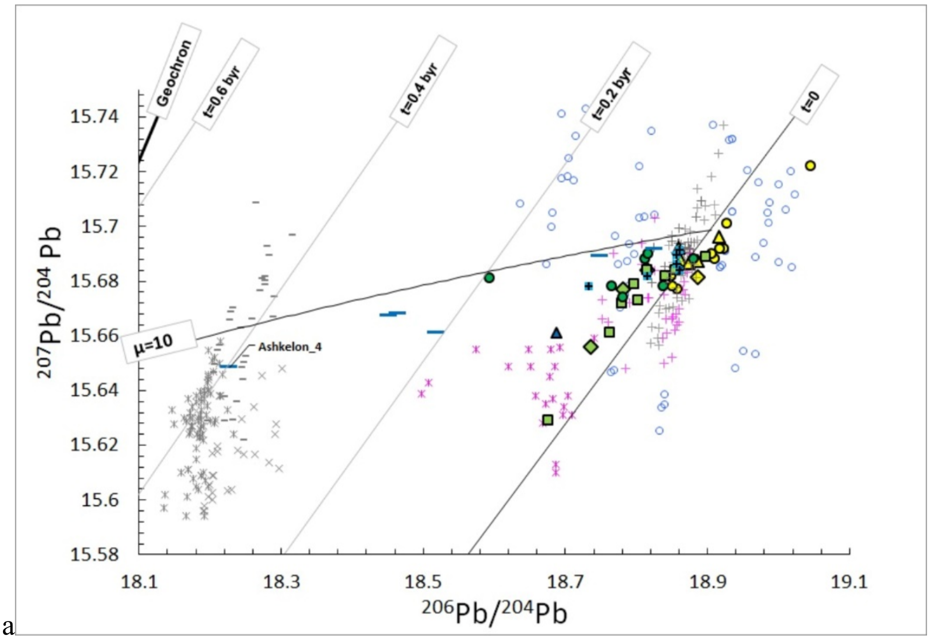

a

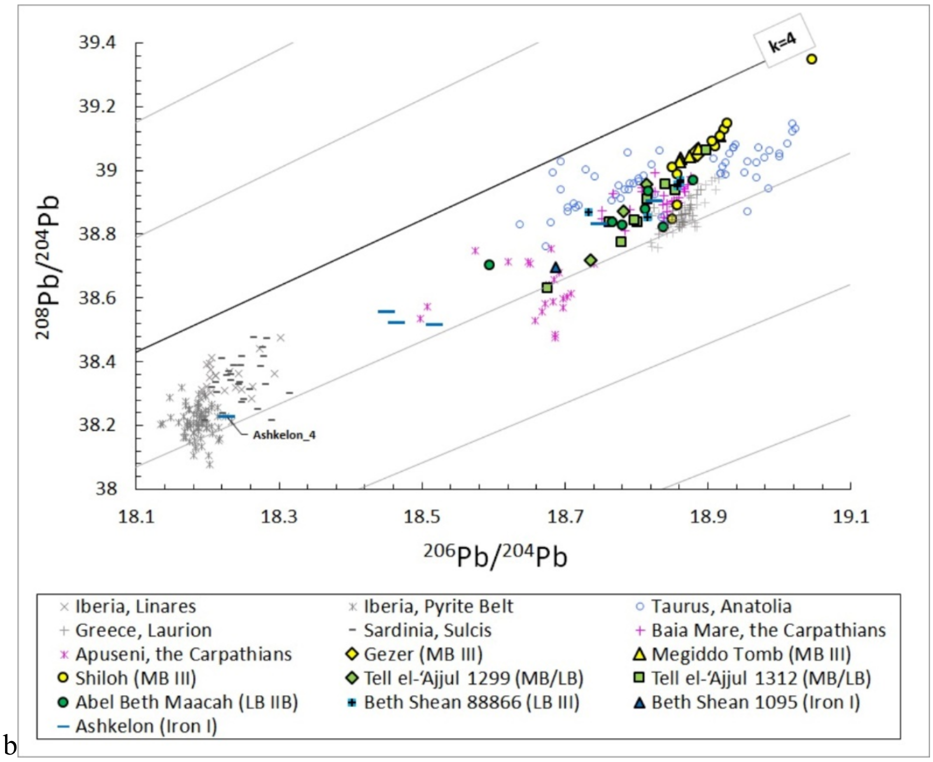

b

Figure S2: (a) $^{207}Pb/^{204}Pb$ vs. $^{206}Pb/^{204}Pb$ of silver items from the Southern Levant analyzed dating to the Middle Bronze Age III (~1700/1650–1600/1550 BC), Middle Bronze/Late Bronze Age transition (~1600/1550–1500 BC), Late Bronze Age IIB (~1300–1200 BC), Late Bronze Age III and Iron Age I (~1200–950 BC). (b) $^{208}Pb/^{204}Pb$ vs. $^{206}Pb/^{204}Pb$ of the same items. Hoards associated to different periods are distinguished by colors: Yellow – Middle Bronze III; Light Green – Middle Bronze/Late

Bronze Age transition; Green – Late Bronze Age II; Blue – Late Bronze Age III and Iron Age I. Ores are in grey (Refs: Anatolia, Taurus: Sayre et al. 1992; Yener et al. 1991; Greece, Laurion: Gale and Stos-Gale 1981b; Stos-Gale and Gale 1982; Vaxevanopoulos et al. 2022; Carpathians: Baron et al. 2011; Marcoux et al. 2002; Iberia, Linares and Pyrite Belt: Murillo-Barroso 2013; Stos-Gale 2001; Tornos and Chiarada 2004; Sardinia, Sulcis: Begemann et al. 2001; Boni and Koeppel 1985; OXALID; Stos-Gale et al. 1995; Valera et al. 2005). Additional ores are excluded from the graphs for simplification. Results obtained from silver-copper alloys were excluded here as well, as the added copper affects LIA by contributing Pb.

Middle Bronze Age III (~1700/1650–1600/1550 BC; yellow symbols in Figure S2)

Silver dating to the MB III derives from two silver hoards from Shiloh in the Central Hill Country of the Southern Levant and Gezer in the *Shephela* (lowlands) and from jewelry from Tomb 50 at Megiddo in the Jezreel valley (Figure 1 in main text). The Pb-isotopic compositions of the majority of the silver items from this period are very similar to each other, suggesting that the silver in them may all have the same origin(s). While the Pb ratios generally fall in the Anatolian-Aegean-Carpathian sphere, the specific source(s) cannot be identified. There are nevertheless two indications that the source(s) should be sought in Anatolia. Firstly, several items in these hoards are stylistically Anatolian, for example a folded silver Cappadocian star, a unique silver pin and a bronze finger axe from the Shiloh hoard (Finkelstein and Brandl 1985), as well as a ray star attached to a crescent pendant from the Gezer hoard (see Eshel et al. 2023, p. 10). Second, the Pb-isotope ratios of the silver are consistent with artefacts from Early Bronze Age Anatolia (Eshel et al. 2023). We thus suggest that most of the silver probably originated there. Two MB III silver items, both from Shiloh, differ isotopically, and are consistent with the ores of Laurion, Greece (Figure S2b), suggesting sporadic and scant connections with the Aegean existed in this period (Eshel et al. 2023). The Carpathians, although consistent isotopically, were probably not reached in this period.

Middle/Late Bronze Age transition (~1600/1550–1500 BC; light green symbols in Figure S2)

The Pb-isotope compositions of MB/LB silver (two hoards from Tell el-ʿAjjul near Gaza in the southern coastal plain) differ from that of the MB III items clearly demonstrating the introduction of silver from new sources to the Levant at this time (Eshel et al. 2023). The results still plot within the Anatolian-Aegean-Carpathian sphere; Some of the silver is consistent with Thasos in the Aegean, however the endmembers are inconsistent with any specific known ores, suggesting that most of the silver may, in fact, be a mix between two or more sources. Two silver bracelet fragments and a pinhead from Tell el-'Ajjul hoard 1312, of Anatolian style, suggest that at least some of the silver originated from Anatolia (Eshel et al. 2023, p. 10).

Comparing the results from Tell el-ʿAjjul to silver from the contemporaneous shaft graves in Mycenae in the Greek Peloponnese, suggests, based on the similar isotopic ratios of the silver, that it may have originated from a common source (Eshel et al. 2023).

Late Bronze Age IIB (~1300–1200 BC; green symbols in Figure S2)

Although the Late Bronze Age II is a period of intensified Mediterranean trade, reaching the Aegean regularly (e.g., Monroe 2015; Murray 2022), only one small silver hoard, with silver ingots and scrap, is known from this period in the Southern Levant (Yahalom-Mack et al. 2019). One item from this hoard, ABM_11, is consistent with Laurion ores, suggesting that some of the silver in the hoard may have been of Greek origin (Figure S2b). The isotopic compositions of the remaining items indicated mixing and a general origin in the Anatolian–Aegean–Carpathian sphere. The silver differs in isotopic composition from the Anatolian MB III silver, but is similar to some of the silver items from the MB/LB transitional phase (Tell el-'Ajjul hoards), and to unalloyed silver from a later hoard from Beth Shean (LB III; see below). This preliminarily observation suggests, albeit on limited data, that the sources of silver to the Levant did not change much throughout the Late Bronze Age.

Late Bronze Age III (~1200–1150 BC; light blue symbols in Figure S2)

The silver dating to the LB III (two silver hoards, one from the Egyptian administrative center at Beth Shean, Locus 88866, and the other from Megiddo, Area H) includes mainly items extensively alloyed with copper, reaching up to 80% of the alloy. We have shown that the likely addition of South Levantine (Arabah)-Cu most likely contributed Pb to the alloy, preventing a straightforward provenance of the silver (Eshel et al. 2021).

Six items in the Beth Shean hoard were produced of unalloyed silver. We previously suggested that they were consistent isotopically with the Laurion mines in Greece (Eshel et al. 2021, p. 6), however, based on the recent observation that the isotopic field of Laurion is more compact than previously assumed (Vaxevanopoulos et al. 2022, p. 23), it appears that the results are inconsistent with the Laurion mines. Although the silver cannot be associated with a specific ore, the results are still consistent with the general Anatolian–Aegean–Carpathian sphere.

Iron Age I (~1150–950 BC; dark blue symbols in Figure S2)

Similarly to the LB III silver, most of the Iron Age I silver was alloyed with copper (four silver hoards from Tell Keisan, Megiddo L2012, Beth Shean 1095 and Ashkelon). Here too, the addition of Cu skews the Pb-isotopic compositions. Only a few silver items from this period were made of pure silver—one item from Beth Shean 1095, and six from Ashkelon—both hoards dating to the *Late* Iron Age I (Eshel et al. 2021). The samples from Ashkelon suggest mixing, having one endmember within the Anatolian–Aegean–Carpathian sphere, the precise origin of which could not be identified; and one that plots against ores that are geologically much older. In fact, for the first time in the history of silver in the Levant, a few samples (n=4) are clearly *in*consistent with Anatolian–Aegean–Carpathian ores (Figure S2). One of these samples (possibly an endmember) is consistent with ores both in Iberia (in the Pyrite Belt near Río Tinto and Linares) and in Sardinia (Sulcis). This may suggest that the beginning of long-distance import of silver to the Southern Levant from the West Mediterranean, which is clearly evident in the subsequent Iron Age II (see below), began as early as the Late Iron Age I (Eshel et al. 2021). Alternatively, it is possible that the six silver items from

Ashkelon were purified by re-heating. In such a case, the isotopic values are indicative of the copper rather than the silver source, and do not indicate the use of western silver at this time. This question is currently unresolved and requires further study and experimentation.

Early Iron Age IIA (~950–900 BC; red symbols in Figure S2)

The Pb-isotope compositions of the silver dating to the Early Iron Age IIA (four silver hoards, from Tel Dor, ʿAkko and two hoards from the 'Southern Palace' at Beth Shean, Locus 1029) form a clear cluster on the graph, consistent with galena from the Taurus mountains, Anatolia. In two of these hoards, from Tel Dor and ʿAkko, another cluster is apparent, consistent with Pb ores in Iglesiente, Sardinia (Eshel et al. 2019; 2022a). This is the earliest clear evidence for the acquisition of silver beyond the Anatolian–Aegean sphere. Many additional isotopic results from these hoards fall on a mixing line between these two endmembers (Taurus and Sardinia), suggesting that silver was often mixed and re-melted. Significantly, in this period, the quality of silver improves substantially and its quantity in the Southern Levant hoards increases (Eshel et al., 2018; 2019; Eshel n.d.).

a

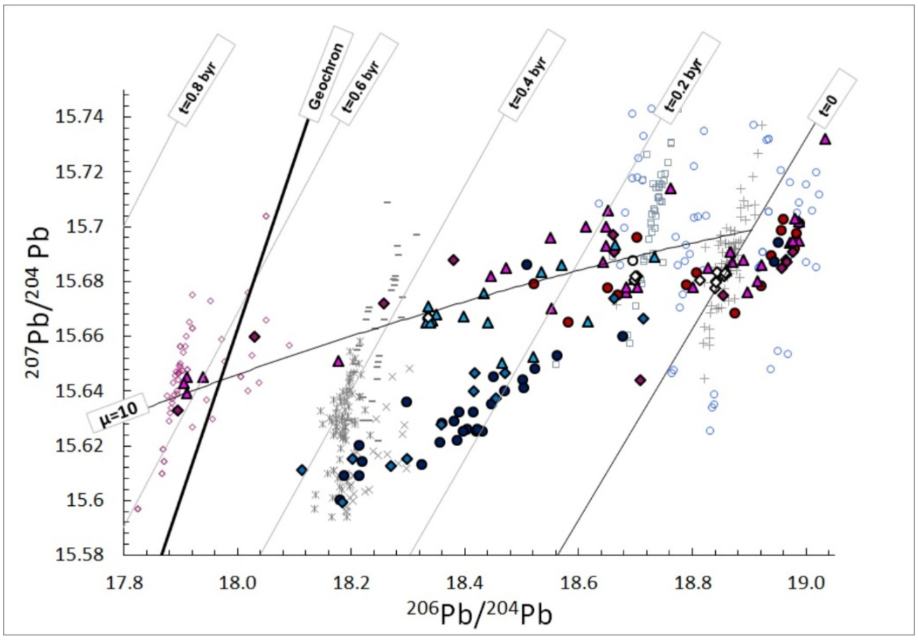

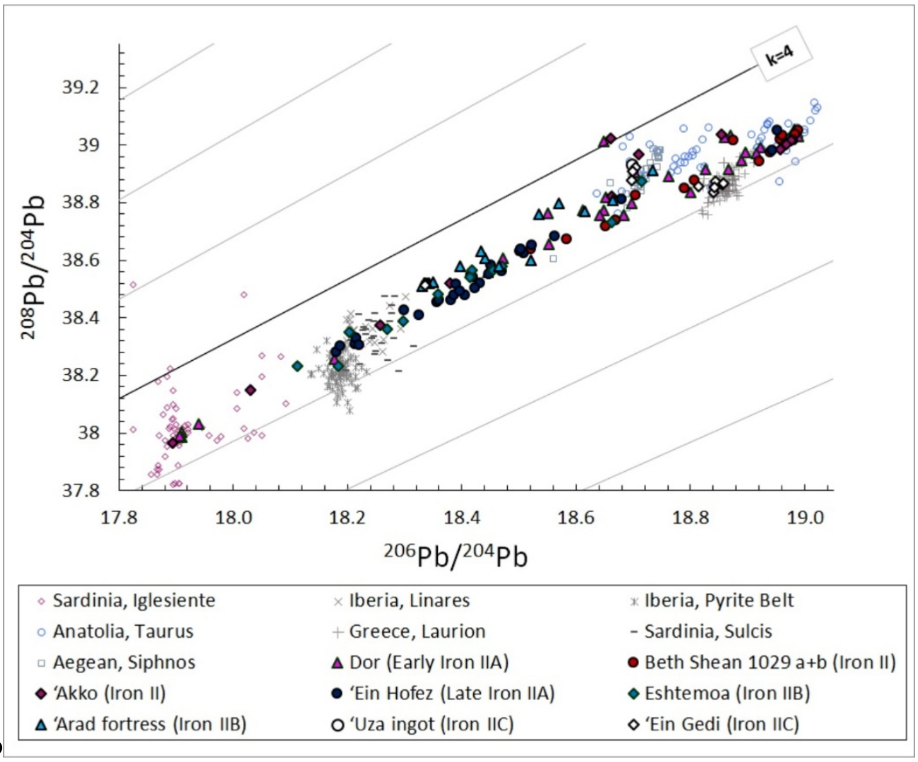

b

Figure S3: (a) $^{207}Pb/^{204}Pb$ vs. $^{206}Pb/^{204}Pb$ of silver items analyzed from the Southern Levant dating to the Early Iron Age IIA (~950–900 BC), Late Iron Age IIA (~900–800 BC), Iron Age IIB (~800–730 BC) and Iron Age IIC (~730–586/600 BC). (b) $^{208}Pb/^{204}Pb$ vs. $^{206}Pb/^{204}Pb$ of the same items. Hoards associated to different periods are distinguished by colors: Red and pink– Early Iron Age IIA and hoards generally dated to the Iron Age II; Blue –Late Iron Age IIA and Iron Age IIB; White –Iron Age IIC. Ores are marked in smaller icons with no fill (Refs: Anatolia, Taurus: Sayre et al. 1992; Yener et al. 1991; Greece, Laurion and Aegean, Siphnos: Gale and Stos-Gale 1981b; Stos-Gale and Gale 1982; Vaxevanopoulos et al. 2022; Iberia, Linares and Pyrite Belt: Murillo-Barroso 2013; Stos-Gale 2001; Tornos and Chiarada 2004; Sardinia, Iglesiente and Sulcis: Begemann et al. 2001; Boni and Koeppel 1985; OXALID; Stos-Gale et al. 1995; Valera et al. 2005. Additional ores are excluded from the graphs for simplification.

Late Iron Age IIA (~900–800 BCE) and Iron Age IIB (~800–730 BC; pink symbols in Figure S3)

This long-time span is represented by one hoard dating to the Late Iron IIA (from ʿEin Hofez) and three Iron Age IIB hoards (from Eshtemoa, ʿArad and Tel Miqne/Ekron [Mikne_5 in OXALID]).

They mostly contain silver consistent with Pb ores from Iberia (Linares and Gador, Almeria), alongside small quantities of silver which is consistent with the Taurus region in Anatolia (Eshel et al. 2022a). The large hoards from ʿEin Hofez (~1.2 kg) and Eshtemoa (~23 kg) and are evidence of the persisting abundance of silver in the Levant during these periods.

Iron Age IIC (~640/630–600 BC; white symbols in Figure S3)

The Pb-isotope ratios of Iron Age IIC silver (one hoard from ʿEin Gedi, an ingot from ʿUza, and five hoards from Tel Miqne/Ekron, all sampled by other scholars (Gentelli et al. 2021; OXALID) are mostly consistent the with the Laurion mines in Attica and the island of Siphnos in the Cyclades, alongside a few items of silver that show consistency with Iberian lead ores (Eshel et al. 2022a).

Bibliography

Albarède, F., Blichert-Toft, J., de Callataÿ, F., Davis, G., Debernardi, P., Gentelli, L., et al. (2021). From commodity to money: The rise of silver coinage around the Ancient Mediterranean (sixth–first centuries BCE). *Archaeometry* **63**: 142—155.

Albarède, F., Blichert-Toft, J., Gentelli, L., Milot, J., Vaxevanopoulos, M., Klein, S., et al. (2020). A Miner's Perspective on Pb isotope Provenances in the Western and Central Mediterranean. *Journal of Archaeological Science* **121**: 105–194.

Albarède, F., Desaulty, A. M. and Blichert-Toft, J. (2012). A Geological Perspective on the use of Pb Isotopes in Archaeometry. *Archaeometry* **54**: 853–867.

Arie, E., Boaretto, E., Martin, M. A., Namdar, D., Shamir, O. and Yahalom-Mack, N. (2019). A New Jewelry Hoard from Eleventh-Century BCE Megiddo. *Near Eastern Archaeology* **82**: 90–101.

Baron, S., Tămaş, C.-G., Cauuet, B. and Munoz, M. (2011). Lead Isotope Analyses of Gold–Silver Ores from Roşia Montană (Romania): A First Step of a Metal Provenance Study of Roman Mining Activity in Alburnus Maior (Roman Dacia). *Journal of Archaeological Science* **38**: 1090–1100.

Baron, S., Tămaş, C.-G. and Le Carlier, C. (2014). How Mineralogy and Geochemistry Can Improve the Significance of P b Isotopes in Metal Provenance Studies. *Archaeometry* **56**: 665–680.

Begemann, F., Schmitt-Strecker, S., Pernicka, E. and Schiavo, F. L. (2001). Chemical Composition and Lead Isotopy of Copper and Bronze from Nuragic Sardinia. *European Journal of Archaeology* **4**: 43–85.

Boni, M. and Koeppel, V. (1985). Ore-Lead Isotope Pattern from the Iglesiente-Sulcis Area (SW Sardinia) and the Problem of Remobilization of Metals. *Mineralium Deposita* **20**: 185–193.

Craddock, P. (2014). Production of Silver Across the Ancient World. *ISIJ international* **54**: 1085–1092.

Eshel, T. (2020). Silver Hoards in the Southern Levant in the Bronze and Iron Ages: Changes in Use and Ore Sources. Ph.D. dissertation, Department of Archaeology, University of Haifa.

Eshel, T. (n.d.). "Keseph": silver-money and the development of a merchant-based economy in the Southern Levant from the Middle Bronze Age to the end of the Iron Age (~2000–600 BCE).

Eshel, T., Erel, Y., Tirosh, O. and Yahalom-Mack, N. (in press). Chemical and isotopic analysis of silver, copper and gold artifacts from Tomb 16/H/50. In Cradic, M. S., Adams M. J., Martin M., and Finkelstein I. (eds.). *Megiddo VII: Decoding Death, The Shmunis Family Foundation's Investigation of Two Elite Bronze Age Tombs, Monograph Series of the Institute of Archaeology*. Tel Aviv University, Eisenbrauns, USA.

Eshel, T., Erel, Y., Yahalom-Mack, N., Tirosh, O. and Gilboa, A. (2019). Lead isotopes in silver reveal earliest Phoenician quest for metals in the west Mediterranean. *Proceedings of the National Academy of Sciences* **116**: 6007–6012.

Eshel, T., Erel, Y., Yahalom-Mack, N., Tirosh, O. and Gilboa, A. (2022a). From Iberia to Laurion: Interpreting Changes in Silver Supply to the Levant in the Late Iron Age Based on Lead Isotope Analysis. *Archaeological and Anthropological Sciences* **14**: 1–24.

Eshel, T., Gilboa, A., Tirosh, O., Erel, Y. and Yahalom-Mack, N. (2023). The earliest silver currency hoards in the Southern Levant: Metal trade in the transition from the Middle to the Late Bronze Age. *Journal of Archaeological Science*, **149**: 105705.

Eshel, T., Gilboa, A., Yahalom-Mack, N., Tirosh, O. and Erel, Y. (2021). Debasement of Silver throughout the Late Bronze – Iron Age Transition in the Southern Levant: Analytical and Cultural Implications. *Journal of Archaeological Science* **125**.

Eshel, T., Tirosh, O., Yahalom-Mack, N., Gilboa, A. and Erel, Y. (2022b). Silver Isotopes in silver suggest Phoenician Innovation in metal production. *Applied Sciences* **12**: 741.

Eshel, T., Yahalom-Mack, N., Shalev, S., Tirosh, O., Erel, Y. and Gilboa, A. (2018). Four Iron Age Silver Hoards from Southern Phoenicia: From Bundles to Hacksilber. *Bulletin of the American Schools of Oriental Research* **379**: 197–228.

Fantalkin, A. and Tal, O. (2015). *Tell Qudadi: an Iron Age IIB Fortress on the central Mediterranean coast of Israel (with references to earlier and later periods); final report on the Hebrew University of Jerusalem excavations*. Peeters.

Finkelstein, I. and Brandl, B. (1985). A group of metal objects from Shiloh. *Israel Museum Journal* **4**: 17–26.

Finkelstein, I., Ussishkin, D. and Cline, E. H. (2013). *"The 2004–2008 Seasons." Megiddo V*. Penn State University Press.

Fischer, P. M. (2021). The last expedition at Tell el-ʿAjjul, Gaza, and the city's final destruction. In: Kamlah, J. and Lichtenberger, A. (eds.), *Palestine and the Mediterranean, Proceedings of the Conference 9th-11th November 2016, Mainz, Organised by the German Society for the Exploration of Palestine*, ADPV.

Gale, N. (2009). A Response to the Paper of AM Pollard: What a Long, Strange Trip it's Been: Lead Isotopes and Archaeology, In Rehren, T. (ed.), *From Mine to Microbe–the Neolithic Copper Melting Crucibles from Switzerland*. pp. 191–196.

Gale, N. H. and Stos-Gale, Z. A. (1981b). Cycladic Lead and Silver Metallurgy. *Annual of the British School at Athens* **76**: 169–224.

Gentelli, L., Blichert-Toft, J., Davis, G., Gitler, H. and Albarede, F. (2021). Metal provenance of Iron Age Hacksilber hoards in the southern Levant. *Journal of Archaeological Science* **134**: 105472.

Gilboa, A. (2015). Dor and Egypt in the Early Iron Age: An Archaeological Perspective of (Part of) the Wenamun Report. *Ägypten und Levante/Egypt and the Levant.* **25**: 247–274.

Gilboa, A. and Sharon, I. (2003). An Archaeological Contribution to the Early Iron Age Chronological Debate: Alternative Chronologies for Phoenicia and their Effects on the Levant, Cyprus, and Greece. *Bulletin of the American Schools of Oriental Research*: **332(1)**: 7–80.

Gilboa, A., Sharon, I. and Bloch-Smith, E. (2015). Capital of Solomon's Fourth District? Israelite Dor. *Levant* **47**: 51–74.

Gilboa, A., Sharon, I., Zorn, J. R. and Matskevitch, S. (2018). *Synthesis, Architecture and Stratigraphy. Excavations at Dor, Final Report: Area G, the Late Bronze and Iron Ages, Qedem Reports*. Jerusalem: Hebrew University.

González de Canales, F., Serrano, L. and Llompart, J. (2008). The Emporium of Huelva and Phoenician Chronology: Present and Future Possibilities, In Sagona, C. (ed.), *Beyond the Homeland: Markers in Phoenician Chronology*. Peeters, Leuven. pp. 631–655.

Gouda, V. K., El-Baradie, Z. M. and Eldamaty, M. (2007). Survey of precious metal production in ancient Egypt. In Argyropoulos, V., Hein, A. and Abdel Harith, M. (eds.). *International Conference on Strategies for Saving Indoor Metallic Collections with a satellite meeting on legal issues in the conservation of cultural heritage*. TEI of Athens. pp. 14–22.

Greenberg, R. (2019). *The Archaeology of the Bronze Age Levant*. Cambridge University Press.

Hauptmann, A. (2007). *The Archaeometallurgy of Copper: Evidence from Faynan, Jordan*. Springer Science & Business Media.

Hofmann, A. (1997). Mantle geochemistry: the message from oceanic volcanism. *Nature* **385 (6613)**: 219–229.

Hofmann, A. (2008). The enduring lead paradox. *Nature Geoscince* **1**: 812–813.

Knapp, A. B. (2000). Archaeology, Science-Based Archaeology and the Mediterranean Bronze Age Metals Trade. *European Journal of Archaeology* **3**: 31–56.

L'Héritier, M., Baron, S., Cassayre, L. and Téreygeol, F. (2015). Bismuth Behaviour During Ancient Processes of Silver–Lead Production. *Journal of Archaeological Science* **57**: 56–68.

Marcoux, E., Grancea, L., Lupulescu, M. and Milési, J. (2002). Lead Isotope Signatures of Epithermal and Porphyry-Type Ore Deposits from the Romanian Carpathian Mountains. *Mineralium Deposita* **37**: 173–184.

Meyers, P. (2003). Production of Silver in Antiquity: Ore Types Identified Based Upon Elemental Compositions of Ancient Silver Artifacts, In Zelst, L. V. (ed.), *Patterns and Process: A Festschrift in Honor of Dr. Edward V. Sayre*. pp. 271–288.

Milot, J., Malod-Dognin, C., Blichert-Toft, J., Télouk, P. and Albarède, F. (2021). Sampling and combined Pb and Ag isotopic analysis of ancient silver coins and ores. *Chemical Geology* **564**: 120028.

Monroe, C. (2015). Tangled up in Blue: Material and Other Relations of Exchange in the Late Bronze Age World, In Howe, T. (ed.), *Traders in the Ancient Mediterranean*. Chicago. pp. 7–46.

Murillo-Barroso, M. (2013). Producción y Consumo de Plata: un Análisis Comparativo Entre la Sociedad Argárica y los Primeros Asentamientos Orientalizantes en el Sur de la Península Ibérica. Ph.D. dissertation. UCL. London.

Murray, S. C. (2022). Eastern Mediterranean Bronze Age Trade in Archaeological Perspective: A Review of Interpretative and Empirical Developments. *Journal of Archaeological Research*. 1–53.

OXALID database: https://oxalid.arch.ox.ac.uk/The%20Database/TheDatabase.htm.

Pernicka, E. (2014). Possibilities and Limitations of Provenance Studies of Ancient Silver and Gold, In Meller, H., Risch, R., and Pernicka, E. (eds). *Metalle der Macht - Frühes Gold und Silber. Metals of Power. Early Gold and Silver. Landesamt für Denkmalpflege und Archäologie Sachsen-Anhalt*. pp. 153–164.

Pernicka, E. (2017). Provenance and Recycling of Ancient Silver. A Comment on "Iridium to Provenance Ancient Silver" by Jonathan R. Wood, Michael F. Charlton, Mercedes Murillo-Barroso, Marcos Martinón-Torres. J. Archaeol. Sci. 81, 1–12. *Journal of Archaeological Science* **86**: 123–126.

Pernicka, E. and Bachmann, H.-G. (1983). Archäometallurgische Untersuchungen zur Antiken Silbergewinnung in Laurion. *Erzmelall* **36**: 592–597.

Pernicka, E., Begemann, F., Schmitt-Strecker, S. and Wagner, G. A. (1993). Eneolithic and Early Bronze Age Copper Artefacts from the Balkans and their Relation to Serbian Copper Ores. *Praehistorische Zeitschrift* **68**: 1–54.

Philip, G. and Rehren, T. (1996). Fourth millennium BC silver from tell esh-Shuna, Jordan: Archaeometallurgical investigation and some thoughts on ceramic skeuomorphs. *Oxford Journal of Archaeology* **15**: 129–150.

Pollard, A. M. (2009). What a Long, Strange Trip it's been: Lead Isotopes and Archaeology, In Rehren, T. (ed.), *From Mine to Microbe–the Neolithic Copper Melting Crucibles from Switzerland*. pp. 181–189.

Pollard, A. and Bray, P. (2015). A New Method for Combining Lead Isotope and Lead Abundance Data to Characterize Archaeological Copper Alloys. *Archaeometry* **57**: 996–1008.

Rehren, T., Hess, K. and Philip, G. (1996). Auriferous silver in western Asia: ore or alloy? *Historical Metallurgy* **30**: 1–10.

Sayre, E., Yener, K. A., Joel, E. and Barnes, I. (1992). Statistical Evaluation of the Presently Accumulated Lead Isotope Data from Anatolia and Surrounding Regions. *Archaeometry* **34**: 73–105.

Schorsch, D. (2001). Precious-metal polychromy in Egypt in the time of Tutankhamun. *The Journal of Egyptian Archaeology*, ***87*****(1)**: 55–71.

Shalvi, G. and Gilboa, A., (2022a). The Last Four Room House in Israel: Stratum 10 at Tel Shiqmona in Context., In Davidovich, U., Matskevich, S., and Yahalom-Mack, N. (eds.), *Material, Method, and Context: Papers on the First Millennium BCE in the Eastern Mediterranean Presented to Ilan Sharon on the Occasion of His Retirement*. Helsinki. pp. 251–312.

Shalvi, G. and Gilboa, A. (2022b). The Long Seventh-Century BCE at Tel Shiqmona (Israel): A High Resolution Chronological Tool for the Levant and the Mediterranean. *Levant* **54**: 190–216.

Shalvi, G. and Gilboa, A. (2023). Between Israel and Phoenicia: The Iron IIA–B Fortified Purple-dye Production Centre at Tel Shiqmona. *Tel Aviv* **50 (1)**: 75–100.

Sharon, I., (2014). Levantine Chronology, In Steiner, M. L. and Killebrew, A. E. (eds.), *The Oxford Handbook of the Archaeology of the Levant: c. 8000-332 BCE.* Oxford University Press. pp. 44–65.

Sharon, I., Gilboa, A., Jull, A. T. and Boaretto, E. (2007). Report on the First Stage of the Iron Age Dating Project in Israel: Supporting a Low Chronology. *Radiocarbon* **49**: 1–46.

Stacey, J. and Kramers, J. (1975). Approximation of Terrestrial Lead Isotope Evolution by a Two-Stage Model. *Earth and Planetary Science Letters* **26**: 207–221.

Stos-Gale, Z. and Gale, N. (1982). The Sources of Mycenaean Silver and Lead. *Journal of Field Archaeology* **9**: 467–485.

Stos-Gale, Z., Gale, N. H., Houghton, J. and Speakman, R. (1995). Lead Isotope Data from the Isotrace Laboratory, Oxford: Archaeometry Data base 1, Ores from the Western Mediterranean. *Archaeometry* **37**: 407–415.

Stos-Gale, Z. A. (2001). The Impact of the Natural Sciences on Studies of Hacksilber and Early Silver Coinage. In Balmuth, M. S. (ed.), *Hacksilber to Coinage: New insights Into the Monetary History of the Near East and Greece: A Collection of Eight Papers Presented at the 99th Annual Meeting of the Archaeological Institute of America*. American Numismatic Society, New York. pp. 53–76.

Toffolo, M. B., Arie, E., Martin, M. A., Boaretto, E. and Finkelstein, I. (2014). Absolute Chronology of Megiddo, Israel, in the Late Bronze and Iron Ages: High-Resolution Radiocarbon Dating. *Radiocarbon* **56**: 221–244.

Tornos, F. and Chiaradia, M. (2004). Plumbotectonic Evolution of the Ossa Morena Zone, Iberian Peninsula: Tracing the Influence of Mantle-Crust Interaction in Ore-Forming Processes. *Economic Geology* **99**: 965–985.

Valera, R. G., Valera, P. and Rivoldini, A., (2005). Sardinian Ore Deposits and Metals in the Bronze Age, In Schiavo, F. L., Giumlia-Mair, A., Sanna, U., and Valera, R. (eds.), *Archaeometallurgy in Sardinia from the Origin to the Beginning of Early Iron Age*, Monique Mergoil. Montagnac. pp. 43–87.

Vaxevanopoulos, M., Blichert-Toft, J., Davis, G. and Albarède, F. (2022). New findings of ancient Greek silver sources. *Journal of Archaeological Science* **137**: 105474.

Wood, J. R., Bell, C. and Montero-Ruiz, I. (2020). The Origin of Tel Dor Hacksilver and the Westward Expansion of the Phoenicians in the Early Iron Age: The Cypriot Connection. *Journal of Eastern Mediterranean Archaeology and Heritage Studies* **8**: 1–21.

Wood, J. R., Montero-Ruiz, I. and Martinón-Torres, M. (2019). From Iberia to the Southern Levant: The Movement of Silver Across the Mediterranean in the Early Iron Age. *Journal of World Prehistory* **32**: 1–31.

Yahalom-Mack, N., Panitz-Cohen, N., Eshel, T. and Mullins., R. (2019). A Late Bronze IIB Silver Hoard from Tel Abel Beth-Maacah*. *Israel Exploration Journal* **69**: 129–153.

Yener, K. A., Sayre, E., Joel, E., Özbal, H., Barnes, I. and Brill, R. (1991). Stable Lead Isotope Studies of Central Taurus Ore Sources and Related Artifacts from Eastern Mediterranean Chalcolithic and Bronze Age Sites. *Journal of Archaeological Science* **18**: 541–577.

Zorn, J. (2014). The Levant during the Babylonian period, In Steiner, M. L. and Killebrew, A. E. (eds.), *The Oxford Handbook of the Archaeology of the Levant: c. 8000-332 BCE*, Oxford University Press.